molecular pharmaceutics

pubs.acs.org/molecularpharmaceutics

Article

The Development of Thermoresponsive Polymeric Simvastatin Prodrug for the Treatment of Experimental Periodontitis in Rats

Xiaoke Xu,[⊥] Zhenshan Jia,[⊥] Ningrong Chen, Subodh M. Lele, Shabnam Arash, Richard A. Reinhardt, Amy C. Killeen, and Dong Wang*

Cite This: *Mol. Pharmaceutics* 2023, 20, 5631−5645

Read Online

ACCESS | Metrics & More | Article Recommendations | Supporting Information

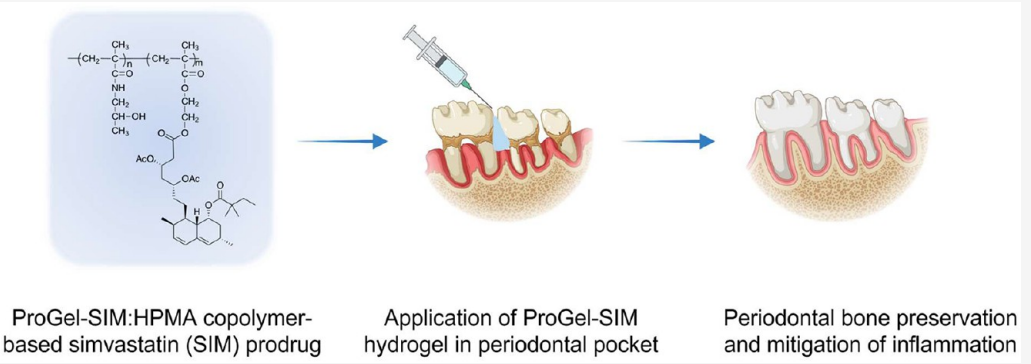

ABSTRACT: Periodontitis (PD) is a severe inflammatory gum pathology that damages the periodontal soft tissue and bone. It is highly prevalent in the US, affecting more than 47% of adults. Besides routine scaling and root planing, there are few effective treatments for PD. Developed as an effective treatment for hyperlipidemia, simvastatin (SIM) is also known for its well-established anti-inflammatory and osteogenic properties, suggesting its potential utility in treating PD. Its clinical translation, however, has been impeded by its poor water-solubility, lack of osteotropicity, and side effects (e.g., hepatoxicity) associated with systemic exposure. To address these challenges, an *N*-(2-hydroxypropyl) methacrylamide (HPMA) copolymer-based thermoresponsive polymeric prodrug of SIM (ProGel-SIM) was developed as a local therapy for PD. Its aqueous solution is free-flowing at 4 °C and transitions into a hydrogel at ∼30 °C, allowing for easy local application and retention. After a thorough characterization of its physicochemical properties, ProGel-SIM was administered weekly into the periodontal pocket of an experimental rat model of PD. At 3 weeks post initiation of the treatment, the animals were euthanized with palate isolated for μ-CT and histological analyses. When compared to dose equivalent simvastatin acid (SMA, active form of SIM) treatment, the rats in the ProGel-SIM treated group showed significantly higher periodontal bone volume (0.34 mm^3 vs 0.20 mm^3, $P = 0.0161$) and less neutrophil (PMN) infiltration ($P < 0.0001$) and IL-1β secretion ($P = 0.0036$). No measurable side effect was observed. Collectively, these results suggest that ProGel-SIM may be developed as a promising drug candidate for the effective clinical treatment of PD.

KEYWORDS: *Prodrug, Thermoresponsive, Hydrogel, Simvastatin, Periodontitis*

INTRODUCTION

Periodontitis (PD) is a widespread and severe periodontal disease that involves the interaction between oral microbiota and host immunity. As the sixth most prevalent disease worldwide, severe PD has an overall prevalence of 11%, with over 743 million people affected.[1] In the US, it affects more than 47% of the adult population. PD is initiated by bacterial infection and the formation of a pathogenic biofilm (plaque). The host immune response induced by dental plaque will damage the periodontal attachment to teeth and the alveolar bone support.[2−4] The main consequence of severe PD is not limited the periodontal bone degeneration and the loss of teeth; it may also result in masticatory dysfunction, malnutrition, cosmetic concerns, and reduced self-esteem.[5] In addition, PD has also been linked to an increased risk of cardiovascular disease, diabetes, and rheumatoid arthritis.[6−8] Current strategies to treat PD involve routine scaling/root planing with the administration of local and systemic antibiotics. Invasive flap surgery and bone graft procedures have been used to repair periodontal bone defects.[9−11] Their moderate efficacy, significant safety risks, and substantial

Received: June 13, 2023
Revised: September 16, 2023
Accepted: September 18, 2023
Published: September 29, 2023

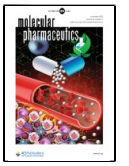

expense, however, have hampered their clinical utilities. Critically, the aforementioned treatment options have limited effects on promoting local bone anabolism and anti-inflammatory activities, two mechanisms that are essential for maintaining periodontal bone quality. Thus, there is a major unmet need for more effective and safe PD therapies.

Statins have been extensively prescribed for hyperlipidemia and cardiovascular diseases.[12−14] As a versatile drug class, they have also been validated for their potent bone anabolic[15−19] and anti-inflammatory[20−23] properties. Specifically, simvastatin (SIM) has been reported to upregulate bone morphogenic protein-2 (BMP-2) expression, induce osteoblast differentiation, and promote mineralization.[15,24,25] It has also been observed with antimicrobial and anti-inflammatory properties.[26,27] Based on their mechanisms of action, the statins, which are commonly prescribed to treat hyperlipidemia, have been considered as a promising drug class for the treatment of PD. The clinical application of SIM in treating PD, however, has been hampered by its poor water-solubility,[28] lack of osteotropicity,[29] and potential complications associated with systemic exposure.[30]

To mitigate these limitations of SIM, we have developed a thermoresponsive polymeric prodrug of SIM (ProGel-SIM) based on *N*-(2-hydroxypropyl)methacrylamide (HPMA) copolymer. The aqueous solution of the thermoresponsive ProGel system[31] is typically a free-flowing liquid at a lower temperature (∼4 °C) and would transition into a hydrogel when exposed to the bodily temperature (∼37 °C), providing an effective strategy for sustained local drug delivery with precision. After a thorough physicochemical characterization of the newly synthesized ProGel-SIM, it was applied in a rat model of PD. The micro-CT and histological data presented in this paper provide robust evidence of alveolar bone preservation and mitigation of local inflammation in rats treated with ProGel-SIM. Furthermore, the evaluation of serum liver function markers suggested that the local application of ProGel-SIM did not affect the normal liver functions of the tested rats, supporting its potential for further development and clinical translation.

MATERIALS AND METHODS

Materials. Simvastatin (SIM) was purchased from Zhejiang Ruibang Laboratories (Wenzhou, Zhejiang, China). Sephadex LH-20 resins were purchased from GE HealthCare (Piscataway, NJ, USA). 2,3-Bis(2-methoxy-4-nitro-5-sulfophenyl)-2*H*-tetrazolium-5-carboxanilide (XTT) cell viability kit (catalog:30007) was purchased from Biotium Inc. (Fremont, CA, USA). ImmPRESS HRP Horse Anti-Rabbit IgG PLUS Polymer IHC Kit (catalog: MP-7801−15) was purchased from Vector Laboratories Inc. (Newark, CA, USA). BMP-2 (catalog: PA585965), IL-1β (catalog: PA5119220), and TNF-α (catalog: PA519810) polyclonal antibodies were purchased from Invitrogen (Carlsbad, CA, USA). Mouse macrophage Raw 264.7 and osteoblast MC3T3-L1 cells were originally purchased from ATCC (Manassas, VA, USA). Dulbecco's modified Eagle's medium (DMEM, catalog: 11965092), Minimum essential medium (MEMα, catalog: 12571063), phosphate buffered saline (PBS, catalog: 20012027), heat-inactivated fetal bovine serum (catalog: 16140071), and 5% penicillin and streptomycin (10,000 U/mL, catalog: 15140122) were purchased from Gibco (Grand Island, NY, USA). Vetscan Comprehensive Diagnostic Profile reagent rotor for blood chemistry analysis was purchased from Abaxis (Union City, CA, USA). All other solvents and chemical reagents, if not specified, were acquired from either Fisher Scientific (Pittsburgh, PA, USA) or Acros Organics (Morris Plains, NJ, USA).

Instruments. ^{1}H and ^{13}C NMR spectra were recorded on a 500 MHz NMR spectrometer (Varian, Palo Alto, CA, USA). Bone samples were analyzed by using a high-resolution Skyscan 1172 Micro-CT system (Bruker, Kontich, Belgium). The number-average molecular weights (M_n), weight-average molecular weights (M_w), and dispersity ($Đ$) of polymeric prodrugs were determined using gel permeation chromatography (GPC) system equipped with a PLgel 5 μm MIXED-C column (Agilent Technologies, Santa Clara, CA, USA), a DAWN 8$^+$ multiangle light scattering (MALS) system (Wyatt Technology Corporation, Santa Barbara, CA, USA), and an Optilab T-rEX refractive index detector (Wyatt). The rheology properties of the ProGel-SIM were assessed by a rheometer (DHR-2 with a 20 mm parallel plate geometry, TA Instrument, USA). The X-ray scattering analyses were performed on a BioSAXS 1000 (Rigaku, Tokyo, Japan) small-angle X-ray scattering (SAXS) system. The images for histological evaluation were acquired with an Aperio CS2 scanning system (Leica, Vista, CA, USA). The absorbance reading for the XTT cell viability assay was obtained by a SpectraMax M2 spectrometer (Molecular Devices, Sunnyvale, CA, USA). The blood chemistry was assessed by using a Vetscan VS2 Chemistry Analyzer (Zoetis, Parsippany, NJ, USA).

Synthesis of the SIM-Containing Monomer. *Synthesis of Compound 1.* Simvastatin (SIM, 4.18 g, 10 mmol), ethylene glycol (12.4 g, 200 mmol), and *p*-toluenesulfonic acid monohydrate (0.38 g, 2 mmol) were dissolved in dichloromethane (DCM, 20 mL). The solution was stirred at room temperature for 2 h. Ethyl acetate (100 mL) was added and washed with brine (100 mL × 3). The organic phase was dried over anhydrous sodium sulfate (Na_2SO_4). The solvent was then removed, and the residue was purified by silica gel column chromatography (mobile phase: ethyl acetate/hexane = 2:1) to give 1.86 g of product, yield: 38.8%.

^{1}H NMR (500 MHz, $CDCl_3$): δ (ppm) = 5.98 (d, J = 9.7 Hz, 1H), 5.78 (dd, J = 9.7 Hz, 6.2 Hz, 1H), 5.49 (br, 1H), 5.37 (d, J = 3.0 Hz, 1H), 4.68 (br, 1H), 4.29 (m, 1H), 4.25 (m, 2H), 4.12 (br, 1H), 3.87 (br, 1H), 3.80 (t, J = 4.5 Hz, 2H), 3.77 (m, 1H), 2.53 (s, 1H), 2.52 (d, J = 1.9 Hz, 1H), 2.44 (m, 1H), 2.37 (dd, J = 11.6 Hz, 5.3 Hz, 1H), 2.24 (dd, J = 11.6 Hz, 2.4 Hz, 1H), 1.95 (m, 1H), 1.94 (m, 1H), 1.50−1.66 (m, 6H), 1.45 (m, 1H), 1.27 (m, 1H), 1.16 (m, 1H), 1.12 (s, 3H), 1.11 (s, 3H), 1.08 (d, J = 7.5 Hz, 3H), 0.87 (d, J = 7.0 Hz, 3H), 0.82 (t, J = 7.5 Hz, 3H). ^{13}C NMR (125 MHz, $CDCl_3$): δ (ppm) = 178.24, 171.97, 132.96, 131.45, 129.35, 128.14, 72.04, 68.85, 68.11, 65.95, 60.31, 42.86, 42.32, 42.22, 37.46, 36.26, 34.80, 32.83(2C), 30.37, 27.11, 24.62, 24.53, 24.15, 22.93, 13.71, 9.16. MS (ESI): m/z = 503.4 (M + Na$^+$), calculated MW = 480.3 g/mol.

Synthesis of Compound 2. Compound **1** (1.80 g, 3.75 mmol) was dissolved in anhydrous DCM (15 mL). Triethylamine (Et_3N, 0.76 g, 7.5 mmol) and 4-dimethylaminopyridine (DMAP, 92 mg, 0.75 mmol) were added, and the solution was cooled to 0 °C using an ice-water bath. Methacryloyl chloride (0.43 g, 4.13 mmol) in DCM (5 mL) was added dropwise. The solution was stirred at 0 °C for 1.5 h. Ethyl acetate (100 mL) was added and washed with brine (100 mL × 3). The organic phase was dried with anhydrous Na_2SO_4. The solvent was then removed, and the residue was purified by silica gel column

https://doi.org/10.1021/acs.molpharmaceut.3c00508
Mol. Pharmaceutics 2023, 20, 5631−5645

chromatography (ethyl acetate/hexanes = 1.5:1) to give 1.83 g of product, yield: 89.2%.

^{1}H NMR (500 MHz, $CDCl_3$): δ (ppm) = 6.13 (s, 1H), 5.98 (d, J = 9.7 Hz, 1H), 5.78 (dd, J = 9.7 Hz, 6.2 Hz, 1H), 5.60 (t, J = 1.6 Hz, 1H), 5.49 (br, 1H), 5.38 (d, J = 3.0 Hz, 1H), 4.39 (m, 4H), 4.27 (m, 1H), 4.11 (br, 1H), 3.80 (br, 2H), 2.52 (d, J = 3.9 Hz, 1H), 2.51 (d, J = 1.5 Hz, 1H), 2.44 (m, 1H), 2.37 (dd, J = 11.6 Hz, 6.2 Hz, 1H), 2.24 (dd, J = 11.6 Hz, 2.4 Hz, 1H), 1.95 (s, 3H), 1.94 (m, 1H), 1.50−1.66 (m, 8H), 1.25 (m, 1H), 1.17 (m, 1H), 1.12 (s, 3H), 1.11 (s, 3H), 1.08 (d, J = 7.5 Hz, 3H), 0.88 (d, J = 7.0 Hz, 3H), 0.82 (t, J = 7.6 Hz, 3H). ^{13}C NMR (125 MHz, $CDCl_3$): δ (ppm) = 177.84, 171.65, 166.92, 135.63, 132.87, 131.42, 129.29, 128.10, 125.98, 71.99, 68.70, 67.89, 62.13, 42.73, 42.19, 41.75, 37.47, 36.06, 34.66, 32.78(2C), 30.29, 27.07, 24.57, 24.46, 24.03, 22.87, 18.04, 13.98, 13.66, 9.09. MS (ESI): m/z = 571 (M + Na^+), calculated MW = 548 g/mol.

Synthesis of Compound ***3***. Compound **2** (1.6 g, 3.0 mmol), Et_3N (0.9 g, 9.0 mmol), and DMAP (0.11 g, 0.9 mmol) were first dissolved in DCM (15 mL), and the solution was then cooled to 0 °C using an ice-water bath. Acetic anhydride (0.77 g, 7.5 mmol) in DCM (5 mL) was added dropwise. The solution was stirred at 0 °C for 1.5 h. Ethyl acetate (100 mL) was added and washed with brine (100 mL × 3). The organic phase was dried over anhydrous Na_2SO_4. The solvent was then removed, and the residue was purified by silica gel column chromatography (ethyl acetate/hexanes = 1:1) to give 1.79 g of product, yield: 94.3%.

^{1}H NMR (500 MHz, $CDCl_3$): δ (ppm) = 6.13 (s, 1H), 5.98 (d, J = 9.7 Hz, 1H), 5.78 (dd, J = 9.7 Hz, 6.2 Hz, 1H), 5.60 (t, J = 1.6 Hz, 1H), 5.49 (br, 1H), 5.38 (d, J = 3.0 Hz, 1H), 5.22 (m, 1H), 4.87 (m, 1H), 4.34 (s, 4H), 2.64 (d, J = 6.9 Hz, 2H), 2.43 (m, 1H), 2.34 (dd, J = 11.6 Hz, 6.2 Hz, 1H), 2.06 (s, 3H), 2.02 (s, 3H), 1.95 (s, 3H), 1.94 (m, 1H), 1.50−1.66 (m, 6H), 1.33 (m, 1H), 1.13 (m, 1H), 1.12 (s, 3H), 1.11 (s, 3H), 1.08 (d, J = 7.5 Hz, 3H), 0.86 (d, J = 7.0 Hz, 3H), 0.82 (t, J = 7.6 Hz, 3H). ^{13}C NMR (125 MHz, $CDCl_3$): δ (ppm) = 177.43, 170.45, 169.92, 169.70, 166.94, 135.79, 132.72, 131.43, 129.63, 128.30, 126.00, 70.97, 67.70, 62.25, 60.26, 42.81, 38.41, 37.57, 37.41, 36.29, 32.85, 32.75, 31.07, 30.39, 27.18, 24.64, 24.58, 23.31, 22.93, 21.08, 20.91, 18.16, 14.10, 13.68, 9.19. (ESI): m/z = 655(M + Na^+), calculated MW = 632 g/mol.

Synthesis of ProGel-SIM. Compound **3** (the SIM-containing monomer, 227 mg, 0.36 mmol), *N*-(2-hydroxypropyl) methacrylamide (HPMA, 200 mg, 1.40 mmol), azobis(isobutyronitrile) (AIBN, 25.2 mg, 0.15 mmol), and RAFT agent *S*,*S*′-bis(α,α′-dimethyl-α′′-acetic acid)-trithiocarbonate (CTA, 24.1 mg, 0.085 mmol) were dissolved in acetone (3.2 mL) in an ampule. The solution was purged with argon for 1.5 min, flame-sealed, and stirred at 55 °C for 48 h. The resulting product was purified with an LH-20 column (mobile phase: methanol) to remove low molecular weight products. After the removal of the solvent, the residue was dissolved in a mixture of water (3 mL) and 1,4-dioxane (5 mL) for lyophilization, yielding 272 mg of ProGel-SIM. The NMR spectra of compounds **1**−**3** and ProGel-SIM are provided in Supporting Information 1.

Characterization of ProGel-SIM. The content of SIM in ProGel-SIM was determined using ^{1}H NMR spectrometry (DMSO-d_6), with trimethyl 1,3,5-benzenetricarboxylate as the internal reference. The chemical shift of the 3 protons on the aromatic ring of trimethyl 1,3,5-benzenetricarboxylate is 8.66 ppm (integration set as 3.00). There is a doublet peak at 5.95 ppm, which belongs to one of the alkene protons. We integrate the peak to determine the molar ratio of SIM and the internal reference. The SIM content in ProGel-SIM was then calculated.

To determine the number-average molecular weights (M_n), weight-average molecular weights (M_w), and dispersity ($Đ$) of ProGel-SIM, the Gel Permeation Chromatography with Multi-Angle Light Scattering Detection (DAWN 8+, Wyatt) and Refractive Index Detection (Optilab T-rEX) system (GPC-MALS) was used. ProGel-SIM was dissolved in dimethylformamide (DMF, ∼2 mg/mL), and the sample (20 μL) was applied to the GPC-MALS equipped with a PLgel 5 μm MIXED-C column (300 × 7.5 mm^2). For the GPC system, the flow rate was set at 0.5 mL/min, the temperature was set at 25.0 °C, and the wavelength of the diode array detector (DAD) was set at 280 nm. For the MALS system, the wavelength of the laser was set at 661 nm. The absolute molecular weight of ProGel-SIM was calculated using ASTRA 7 software.

Construction of the Phase Transition Diagram of ProGel-SIM. The tube-tilting method[32] was used to construct the solution−hydrogel−syneresis (*sol*−*gel*−*syn*) phase transition diagram of the ProGel-SIM solution with different concentrations and SIM contents. Briefly, Eppendorf tubes (1.5 mL) containing an aqueous solution of ProGel-SIM (0.2 mL) were placed in a dry block heater with precise temperature control (Multi-Block Digital Dry Incubator 2002, Thermo Scientific, USA). A thermometer with an accuracy of 0.1 °C was immersed in 1.5 mL Eppendorf tubes containing 0.5 mL of water to indicate the temperature change. The *sol*−*gel* transition temperature of each ProGel-SIM sample ([SIM] = 22 w/w %, 24 w/w %, and 26 w/w %) was determined by flow or no flow criterion over 30 s with the test tube inversion, and the *gel*−*syn* transition temperature was determined at the point when a thin water layer was observed on the top the gel. The transition temperature was monitored with an accuracy of ±1 °C.

Analysis of the Rheological Properties of ProGel-SIM. Rheology study of the ProGel-SIM ([SIM] = 26 w/w %; [ProGel-SIM] = 20 w/v %) was performed by using a DHR-2 rheometer with a 20 mm parallel plate geometry (TA Instrument, USA). The sample was uniformly loaded between the Peltier plate of the rheometer by using a syringe, and the sample thickness was set at 500 μm. The linear viscoelastic range (LVR) was predetermined at 30 °C by using the oscillation amplitude function, with the following condition: strain of 0.5% and angular frequency of 10 rad/s. The rheological parameters used in all tests were within LVR. The temperature for phase changes was determined by measuring the storage modulus (G') and loss modulus (G'') of samples in the oscillation temperature ramp (10−40 °C) with a heating rate of 1 °C/min.

Erosion Behavior of ProGel-SIM. The erosion kinetics of the ProGel-SIM ([SIM] = 22 w/w %, 24 w/w %, 26 w/w %) was assessed by measurement of the remaining gel weight (%) during incubation. The concentration for ProGel-SIM with SIM content of 24 w/w % and 26 w/w % was set at 15 w/v %; and for ProGel-SIM with SIM content of 22 w/w %, the concentration was set at 25 w/v %. The samples were prepared with 0.9% saline in 2 mL Eppendorf tubes and formed the gel at 37 °C. Each empty tube's weight was measured as W_0, and the original total weight with the addition of ProGel-SIM was measured as W_{G0}. Phosphate-buffered saline (PBS, pH 6.6, 200

https://doi.org/10.1021/acs.molpharmaceut.3c00508
Mol. Pharmaceutics 2023, 20, 5631−5645

μL) pre-equilibrated at 37 °C was gently added on top of the ProGel-SIM. The Eppendorf tube was then incubated at 37 °C in a water bath with continuous gentle shaking at ~50−60 rpm/min. After careful removal of the supernatant, the weight of the remaining ProGel-SIM together with the Eppendorf tube was measured as W_{Gt} at predetermined time intervals (12, 24, 48, 1, 3, and 7 days), followed by the addition of fresh buffer (200 μL). The remaining weight (%) and weight loss (%) of the ProGel-SIM were calculated using the following formulas and plotted vs the incubation time:

$$\textit{Remaining Weight}\ (\%) = \frac{W_{Gt} - W_0}{W_{G0} - W_0} \times 100$$

$$\textit{Weight Loss}\ (\%) = \frac{W_{G0} - W_{Gt}}{W_{G0} - W_0} \times 100$$

Small-Angle X-ray Scattering (SAXS) Analysis of ProGel-SIM. The aqueous solution of 15% w/v ProGel-SIM ([SIM] = 24 w/w %) was prepared in water of HPLC grade. The X-ray SAXS profiles of ProGel-SIM were collected at different temperatures (5, 15, 25, 35, 45 °C). After subtracting the water signal, scattering profiles of ProGel-SIM were analyzed with ATSAS (Version: 3.1.3, EMBL, Hamburg)[33] and RAW BioSAXS (Version: 2.1.1). The Guinier analysis at the low q region was first determined to get the initial radius of gyration (R_g). Because ProGel-SIM is a polydisperse system, the indirect Fourier transform (IFT) method was implemented by the GNOM (Version 4.6 ATSAS team 1991−2009) to obtain the distribution of R_g and maximum diameter (D_{max}) for the ProGel-SIM system at different temperature. From the analyses, the $P(r)$ function, the fit line, and the fit residual were also obtained.

Analysis of the Potential Cytotoxicity of ProGel-SIM. Mouse macrophage Raw 264.7 and osteoblast MC3T3-L1 cell lines were cultured in Dulbecco's modified Eagle's medium (DMEM) and Minimum Essential Medium (MEMα), respectively. The media were supplemented with 10% fetal bovine serum (FBS) and 1% penicillin−streptomycin. Cells were incubated at 37 °C with 5% CO_2 to 90% confluence prior to the cytotoxicity study. 2,3-Bis(2-methoxy-4-nitro-5-sulfophenyl)-2*H*-tetrazolium-5-carboxanilide (XTT) cell viability kit was used in this study according to the protocol provided by the manufacturer. Briefly, RAW 264.7 and MC3T3-L1 cells were seeded in 96-well plates (1×10^4 cells/well) and treated with ProGel-SIM and Simvastatin acid sodium salt (SMA, active form of SIM), respectively, for 24, 48, and 72 h. The drug solutions were prepared with cell culture medium at different concentrations (100 nM to 50 μM, SIM equivalent). The cells without any treatment were set as a blank control. Following each time point, 50 μL of XTT solution was added to each well and further incubated for 6 h at 37 °C. The UV absorbance of each well was measured at 450 nm using a SpectraMax M2 spectrometer (Molecular Devices, Sunnyvale, CA, USA). The cell viability was calculated by using the following equation:

$$\textit{Cell viability}\ (\%) = \frac{OD_s}{OD_c} \times 100$$

where OD_c is the optical density of the untreated cells, and OD_s is the optical density of the treated cells. Experiments were repeated five times for each concentration at each time point. As the control treatment, SMA was synthesized in-house according to the literature[34] with slight modifications. Briefly, SIM (1 mmol) and sodium hydroxide (1 mmol) were dissolved in acetone (3 mL) and water (3 mL), respectively. The two solutions were mixed and incubated at room temperature for 10 min. After the removal of acetone, the product was washed thoroughly with ethyl acetate and water. The water layer was then lyophilized to produce SMA (0.307 g, purity >97%, HPLC).

Animal Experiment. Sprague−Dawley rats (female, 11-month-old, retired breeders) were purchased from Envigo (Indianapolis, IN, USA). Experimental PD was induced by placing 4−0 silk ligatures between the maxillary first molar (M1) and second molar (M2).[35,36] After the ligatures placement, rats were randomized into four groups (8 rats/group), which included Healthy, ProGel-SIM treated ([ProGel-SIM] = 25 w/v%; [SIM] = 26 w/w%), SMA treated, and Saline groups. The Healthy rats were intact without ligature placement and were used as a positive control group. At 1 week post-PD induction, the ligatures were removed from the animals. ProGel-SIM (10 μL, 0.39 mg of SIM equivalent) and SMA (10 μL, 0.39 mg of SIM equivalent) were injected locally between M1 and M2 from both the lingual and buccal side of palatal gingiva weekly. Saline (10 μL) was administered in a fashion similar to that of a negative control. Three weeks later, all the animals were euthanized, and the entire palate with maxillary dentitions was collected and fixed in 10% formalin prior to microcomputed tomography (μ-CT) and histological analysis. All procedures were performed according to a protocol approved by the Institutional Animal Care and Use Committee (IACUC) of the University of Nebraska Medical Center and conducted following the National Institutes of Health Guide for the Care and Use of Laboratory Animals.

Microcomputed Tomography (μ-CT) Analysis. The palates were scanned by using a high-resolution μ-CT system (Skyscan 1172) with the following scanning parameters. The X-ray tube voltage and current were set at 70 kV and 141 μA, respectively; a 0.5 mm thick aluminum filter was used to improve imaging quality; exposure time was set at 720 ms; and the X-ray projections were obtained at 0.7° intervals with a scanning angular rotation of 180°, and five frames were averaged for each rotation. Reconstructions were performed afterward to establish three-dimensional (3D) structures by using NRecon software. For quantitative analysis, the position of each palate was corrected, and the sagittal and coronal images were saved separately using DataViewer (Version 1.5.6.2). To obtain the histomorphometric parameters, a rectangular region of interest (ROI) between M1 and M2 was chosen, which was identified as distopalatal of M1 to the mesiopalatal of M2 (length) and from palatal to buccal sides of M1 and M2 (width). This rectangular ROI was carefully placed below the cementoenamel junction (CEJ) of M1 and M2 for 150 slices. Subsequently, a custom analysis was performed using CTan (ver. 1.16.4.1) to determine the histomorphometric parameters such as bone volume (BV), bone volume fraction (BV/TV), trabecular thickness (Tb.Th), and trabecular separation (Tb.Sp) for each palate sample. To evaluate bone erosion, the distance from the CEJ to an alveolar bone crest (ABC) between M1 and M2 was also measured in the sagittal images. The measurement was performed ten times for each side of the palate using CTan, and mean values were calculated. To better visualize the extent of periodontal bone erosion, the 3-D images of each palate sample were generated using CTvox.

https://doi.org/10.1021/acs.molpharmaceut.3c00508
Mol. Pharmaceutics 2023, 20, 5631−5645

Scheme 1. Synthesis of ProGel-SIM

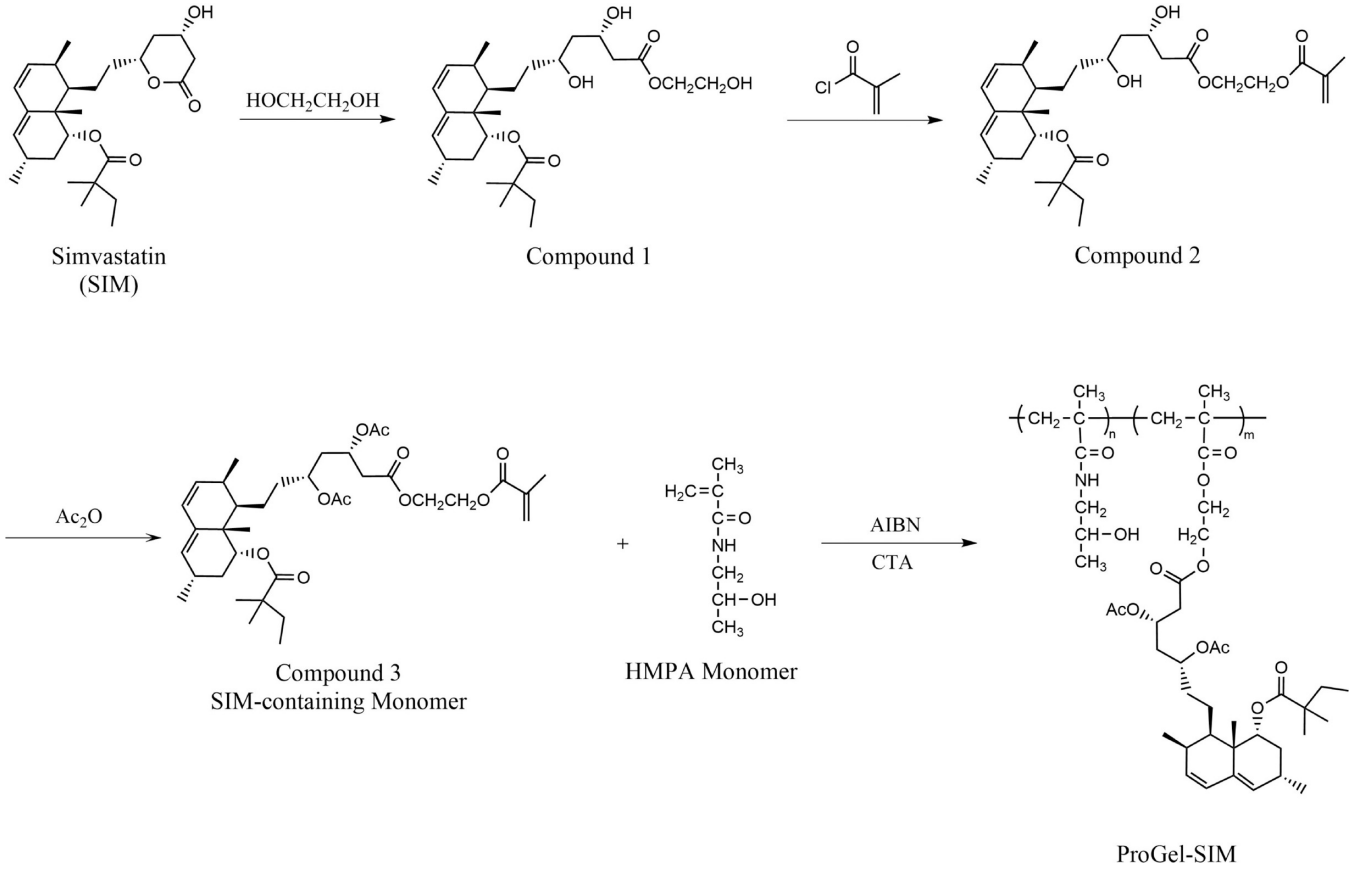

Histological Analysis. After μ-CT analysis, the palates of the rats were decalcified for 2 weeks using a 10% EDTA solution. Following decalcification, the tissues were rinsed in PBS for 12 h to eliminate the remaining EDTA and then dehydrated (70% ethanol, 80% ethanol, 95% ethanol, 100 ethanol, Histo-clear, paraffine) for embedding. After tissues were embedded in paraffin, the sagittal sections (at 5 μm thick) were obtained using a Leica microtome (Wetzlar, Germany). The hematoxylin and eosin (HE) staining and immunohistochemistry (IHC) were subsequently performed to evaluate the leukocytes infiltration, the levels of inflammatory cytokines (IL-1β and TNF-α) secretion, and the levels of BMP-2 expression. For HE staining, the sections were stained with hematoxylin and eosin for 5 and 2 min, respectively. A commercially available kit (ImmPRESS HRP Horse Anti-Rabbit IgG PLUS Polymer IHC Kit) was used for IHC, following the procedure provided by the manufacturer. The antirat IL-1β, TNF-α, and BMP-2 antibodies were diluted in 2.5% normal horse serum with a ratio of 1:30, 1:1000, and 1:200, respectively, and incubated with the samples overnight. All histological images were captured by a Leica Aperio CS2 scanning system at 200× or 400× magnification for scoring and semiquantification. The neutrophil and lymphocyte infiltration into the connective tissue between M1 and M2 was scored by a pathologist (SML) who was blinded to the grouping design. The scoring system was defined as follows: 0 is negative; 1 is less than 30% of the affected tissues; 2 is some inflammatory cells (30%−60%); and 3 is many inflammatory cells (>60%). The expression levels of IL-1β, TNF-α, and BMP-2 in the connective tissue between the M1 and M2 were quantitatively analyzed by using ImageJ.[37]

Hepatic Function Assessment. The hepatic function of the rats was evaluated by analyzing three serum markers, including alanine aminotransferase (ATL), albumin (ALB), and alkaline phosphatase (ALP). The whole blood was collected from rats on the day of euthanasia by using the heart puncture method, and the serum was separated from the whole blood by a refrigerated centrifuge (4 °C and 2000 rpm for 20 min). The serum (100 μL) was loaded onto the Vetscan Comprehensive Diagnostic Profile reagent rotor (Abaxis, CA, USA) and then analyzed by Vetscan VS2 Chemistry Analyzer (Zoetis, NJ, USA) to quantitatively determine the serum level of ALT, ALB, and ALP for the rats in each treatment group.

Statistical Analysis. All data were presented in the format of mean ± standard deviation (SD). The unpaired parametric t test was performed to analyze the data obtained from the cytotoxicity study. The Mann−Whitney U test was performed for the analyses of pathological scores. The P value was determined by a two-tailed t test and a Mann−Whitney U test. The continuous outcomes among more than two groups were compared using one-way analysis of variance (ANOVA) with Tukey's *post hoc* analysis for multiple comparisons in bone analysis. All of the analyses were performed using GraphPad Prism 9.0 (GraphPad, San Diego, CA). Differences were considered statistically significant when $P < 0.05$.

RESULTS

Synthesis of ProGel-SIM. The thermoresponsive polymeric prodrug of simvastatin (ProGel-SIM) was successfully synthesized according to the route illustrated in Scheme 1. The lactone ring of SIM was opened with ethylene glycol. The resulting primary hydroxyl group then reacted with meth-

https://doi.org/10.1021/acs.molpharmaceut.3c00508
Mol. Pharmaceutics 2023, 20, 5631−5645

Table 1. Characterization of the ProGel-SIM

SIM contents (w/w %)	M_w (g/mol)	M_n (g/mol)	$Đ$
22.00	8.65×10^3 (±9.20%)	7.37×10^3 (±8.26%)	1.17 (±12.40%)
23.78	8.50×10^3 (±7.72%)	7.39×10^3 (±7.70%)	1.15 (±10.91%)
26.20	8.52×10^3 (±9.29%)	7.16×10^3 (±8.56%)	1.19 (±12.64%)

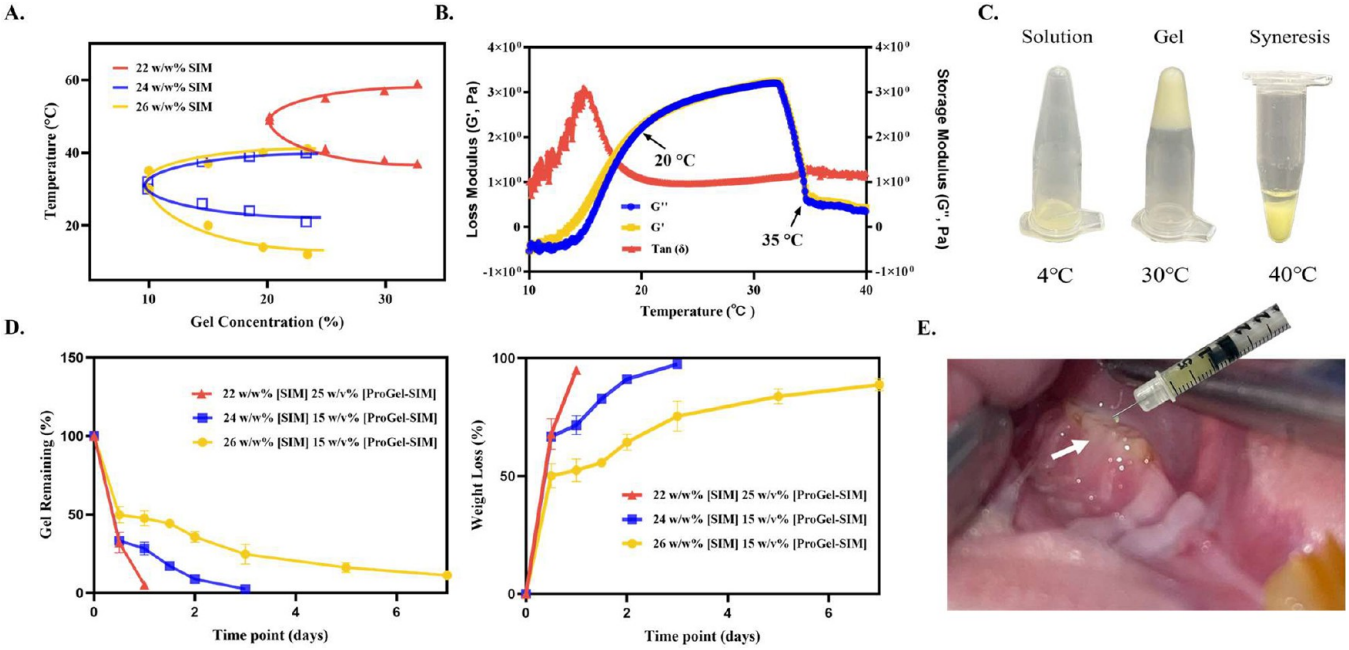

Figure 1. Thermoresponsive property of ProGel-SIM. (A) The *sol*−*gel*−*syn* phase transition diagram of ProGel-SIM with 22 w/w %, 24 w/w %, and 26 w/w % SIM content. (B) The temperature ramp was performed with an elevation of temperature from 10 to 40 °C to determine the storage modulus (G'), loss modulus (G''), and their ratio (tan δ) of 20 w/v % [ProGel-SIM] with 26 w/w % [SIM] content. (C) The appearance of ProGel-SIM at 4, 30, and 40 °C. Left image: free-flowing ProGel-SIM solution at 4 °C; middle image: ProGel-SIM hydrogel at 30 °C; right image: ProGel-SIM in the syneresis phase. (D) The gel remaining (left) and the weight loss (right) of the 25 w/v % or 15 w/v % [ProGel-SIM] with 22 w/w %, 24 w/w %, and 26 w/w % [SIM]. (n = 3) Data are expressed as mean ± SD. (E) The ProGel-SIM could be easily injected through an insulin syringe and formed the gel (white arrow) instantly at the periodontal pocket.

acryloyl chloride to produce a SIM-containing hydroxyethyl methacrylate (HEMA) monomer (HEMA-SIM). To avoid spontaneous reclosure of the SIM's lactone ring during its polymerization, the two secondary hydroxyls of HEMA-SIM were masked with acetyl groups. In addition to stabilization of the monomer, the masking of the secondary hydroxyls may also improve the membrane permeability of the drug.[38] The resulting SIM-containing monomer was subsequently RAFT copolymerized with HPMA in acetone to produce a thermoresponsive polymeric prodrug for simvastatin (ProGel-SIM). This simple synthetic route holds promise for future large-scale manufacturing. In the current ProGel-SIM design, carboxylic ester linker chemistry was used as the ProGel-SIM activation trigger. Once administered, esterase catalyzes the hydrolysis of ProGel-SIM, resulting in sustained SIM activation and release.

Characterization of the ProGel-SIM. Given the presence of several pH-sensitive groups in the ProGel-SIM structure, acid-mediated complete prodrug activation will not only release SIM but also produce additional SIM-derivatives, which would complicate the quantification of the SIM content in ProGel-SIM using the conventional HPLC method. Therefore, ^{1}H NMR was used to determine the SIM content in ProGel-SIM. Using trimethyl 1,3,5-benzenetricarboxylate as the internal calibration, the actual SIM contents for three batches of ProGel-SIM were determined as 22 (22.00) w/w %, 24 (23.78) w/w %, and 26 (26.20) w/w %. Using the GPC-MALS system, the M_w, M_n, and $Đ$ of these ProGel-SIM were also determined and are shown in Table 1.

Thermoresponsive Behaviors of ProGel-SIM. In our initial assessment of ProGel-SIM ([SIM] = 26 w/w %; [ProGel-SIM] = 15 w/v %), its aqueous solution was observed to be a free-flowing liquid at 4 °C but formed a hydrogel when the temperature was elevated to ∼30 °C. In addition, we also observed that there was a thin layer of water on the top of the gel when the temperature elevated to ∼40 °C (Figure 1C), which indicated syneresis. Given the significance of the thermoresponsive property of ProGel-SIM for its potential *in vivo* applications, we conducted a series of studies to fully comprehend the thermoresponsive phase transition behavior. The test tube tilting method was used to measure solution-hydrogel-syneresis (*sol*−*gel*−*syn*) transition temperatures of ProGel-SIM with different SIM contents and at different concentrations, producing the phase-transition diagrams as plotted in Figure 1A. The ProGel-SIM with higher SIM content showed lower *sol*−*gel* transition temperatures. With the decrease in concentration, its *sol*−*gel* transition temperatures were approaching its *gel*−*syn* transition temperatures, which was consistent with our previous observation in a different ProGel system.[31] The ProGel-SIM with the lowest drug loading (22 w/w %) had a relatively high gelation temperature when compared to the ProGel-SIM with drug

https://doi.org/10.1021/acs.molpharmaceut.3c00508
Mol. Pharmaceutics 2023, 20, 5631−5645

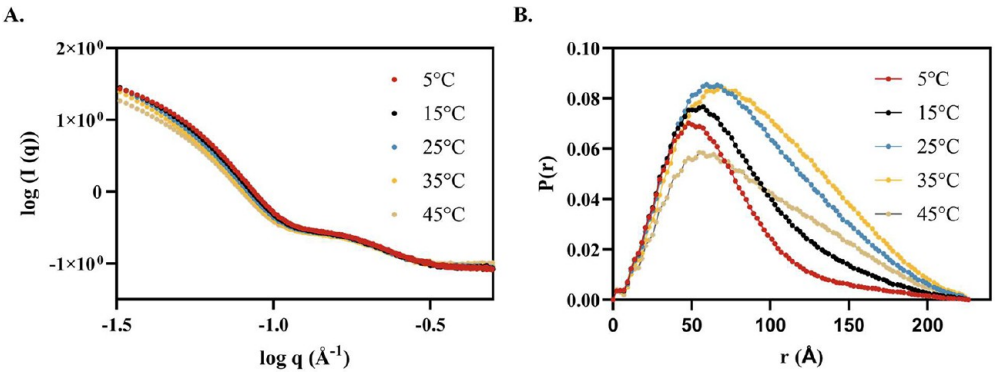

Figure 2. Scattering profiles of ProGel-SIM at different temperatures. Small-angle X-ray analysis (SAXS) for ProGel-SIM at different temperatures was performed. The one-dimensional scattering curves at different temperatures were implemented by GNOM (an indirect Fourier transform for SAXS data processing) to calculate the R_g and D_{max} values. (A) The raw scattering data were plotted as log(q) vs log ($I(q)$) for the ProGel-SIM at different temperatures. (B) The size distribution of the ProGel-SIM at different temperatures was shown by calculating the $P(r)$ function.

loading of 24 and 26 w/w %. Its T_{Gel} was at ∼40 °C even with high ProGel-SIM concentration (25 w/v %). When the ProGel-SIM concentration was reduced to <20 w/v %, it would not form gel even at 60 °C.

The storage modulus (G'), loss modulus (G''), and their ratio (Tan δ) of the ProGel-SIM were evaluated with a rheometer (Figure 1B). We found that both G' and G'' increased with the elevation of the temperature, but the G'' was prominently larger than the G' below 21.38 °C, indicating that the rheological behavior of ProGel-SIM ([SIM] = 26 w/w % [ProGel-SIM] = 20 w/v %) was more plastic than elastic. With the elevation of temperature from 21.38 to 34.84 °C, the G' was gradually overlapping with the G''. In some temperature ranges (21.8 to 27.3 °C), the value of G' was slightly larger than G'', and in some temperature ranges (27.3 to 34.84 °C), the value of G' was slightly smaller than G''; however, the differences between G' and G'' was not prominent. The *sol–gel* transition will lead to the value of G' significantly exceeding that of G'', but it was not observed in the ProGel-SIM system. We assumed the potential reason for this rheological behavior of ProGel-SIM is that it is a soft material; therefore, in the gelation process, even with small strains (0.5%) applied, water would be easily squeezed out of hydrogel, which was detected by the rheometer leading to the similar G' and G'' values at the gelation temperature.

Erosion of ProGel-SIM. The *in vitro* gel erosion test was conducted to assess the erosion kinetics of ProGel-SIM with SIM contents of 22 w/w %, 24 w/w %, and 26 w/w % in a simulated environment of the periodontal pocket (pH ≈ 6.6).[39,40] The ProGel-SIM with different SIM contents showed different gel erosion kinetics, and the erosion rate was negatively correlated with the SIM content (Figure 1D). Specifically, the ProGel-SIM with higher SIM content eroded slower than the ProGel-SIM with lower SIM content. The ProGel-SIM with the lowest drug loading (22 w/w %) eroded very quickly within 24 h, which is probably not suitable for *in vivo* use and clinical translation. With the overall considerations of SIM content, gelation temperature, and gel erosion kinetics, we decided to use the 15 w/v % ProGel-SIM with 26 w/w % SIM content for the *in vivo* study.

Small-Angle X-ray Scattering Analysis of ProGel-SIM. SAXS is commonly used to analyze the structures of biomacromolecules, polymers, and colloids. The technique is accurate and nondestructive.[41,42] Therefore, it was used to probe the changes in the ProGel-SIM hydrogel's inner structure at different temperatures. The result may help to reveal the mechanism responsible for the thermoresponsive phase transition process. The initial scattering profile is shown in Figure 2A, based on which the size distribution, radius of gyration (R_g), and largest diameter (D_{max}) of ProGel-SIM at different temperatures were determined (Figure 2B and Table 2). The R_g and D_{max} continuously increased with the elevation of the temperature from 5 to 35 °C (R_g: 52.59 ± 0.21 nm to 70.73 ± 0.75 nm; D_{max}: 197–246 nm) but dropped when the temperature reached 45 °C (R_g: 59.89 ± 0.45 nm; D_{max}: 209 nm).

Table 2. R_g and D_{max} of ProGe-SIM at Different Temperatures

Temperature (°C)	R_g (Å)[a]	D_{max} (Å)[a]	Fitting Error
5	52.59	197	0.21
15	55.97	212	0.40
25	63.52	231	0.82
35	70.73	246	0.75
45	59.89	209	0.45

[a]The values of R_g and D_{max} of the ProGel-SIM at different temperatures were generated by fitting the scattering profile into the GNOM program (Version 4.6 ATSAS team 1991–2009).

ProGel-SIM Exhibited No Cytotoxicity in the Murine Macrophage and Osteoblast Culture Systems. HPMA copolymers are known to have excellent biocompatibility.[43] SIM has also been used for several decades as a safe medication for hyperlipidemia.[12,44] Therefore, we posit that the newly synthesized ProGel-SIM as a polymeric prodrug for SIM would exhibit an excellent safety profile. To confirm our speculation, mouse macrophage RAW 264.7 (Figure 3A) and osteoblast MC3T3-L1 (Figure 3B) cell lines were treated with ProGel-SIM (100 nM to 50 μM, SIM equivalent) and Simvastatin acid (SMA, 100 nM to 50 μM, SIM equivalent) for 24, 48, and 72 h. At the end of the first 24 h, the cell viability was about 100% for both ProGel-SIM and SMA treatments at all concentrations, suggesting their lack of cytotoxicity to the two cell lines with short-term exposure. The cell viability was significantly compromised, however, at higher concentrations of SMA (10 and 50 μM treatment) after 48 and 72 h of incubation, suggesting toxicity with long-term SMA exposure. For cell lines treated with ProGel-SIM, however, they maintained ∼100% viability at all tested concentrations even

https://doi.org/10.1021/acs.molpharmaceut.3c00508
Mol. Pharmaceutics 2023, 20, 5631–5645

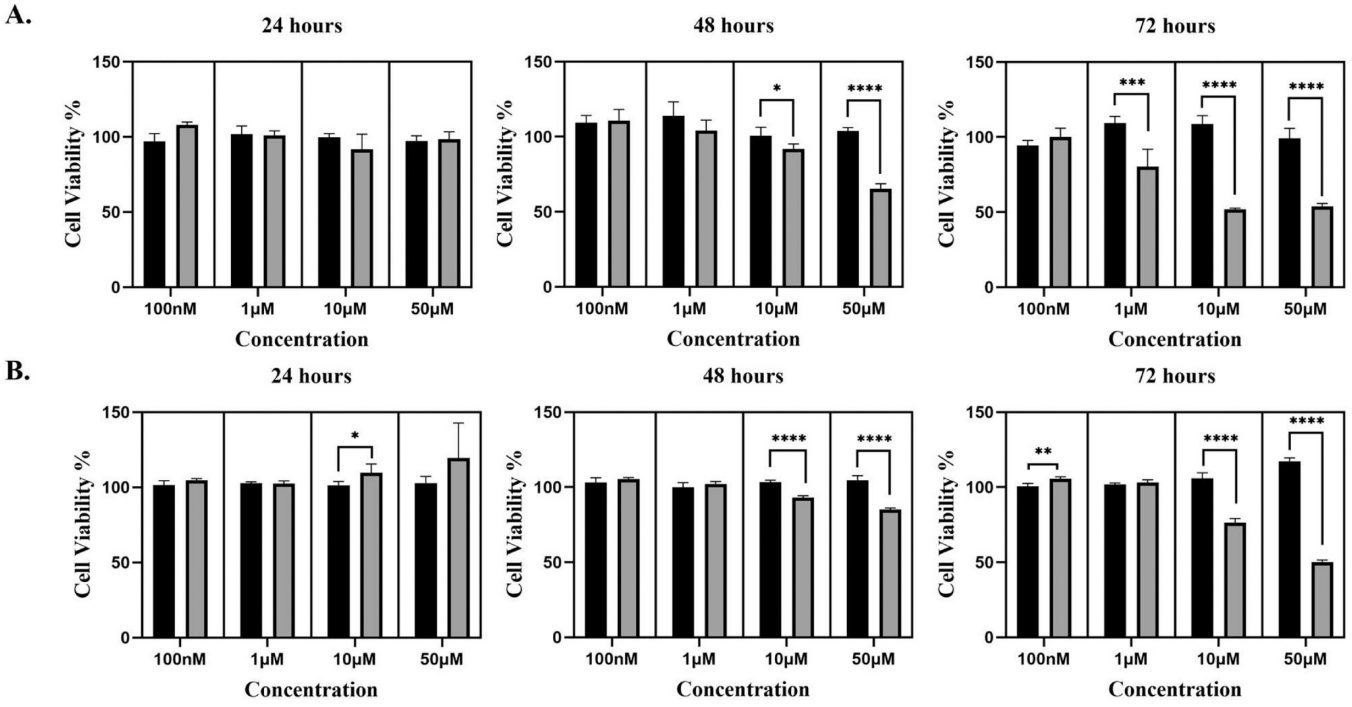

Figure 3. *In vitro* cell viability test of ProGel-SIM and SMA in Raw 264.7 and MC3T3-L1 cell lines. The cytotoxicity of ProGel-SIM (black) and SMA (gray) in (A) Raw 264.7 and (B) MC3T3-L1 cell lines after 24, 48, and 72 h treatment (n = 5 for each treatment). Data are expressed as mean ± SD * $P < 0.05$; ** $P < 0.01$; *** $P < 0.001$; **** $P < 0.0001$ (unpaired parametric t test).

after 72 h of exposure, confirming its excellent safety/biocompatibility.

Local Application of ProGel-SIM Mitigates Periodontitis and Associated Alveolar Bone Loss. Alveolar bone loss associated with chronic inflammation is one of the major manifestations of severe PD. To assess the periodontal bone preservation and regeneration capacity of ProGel-SIM, we administered ProGel-SIM ([SIM] = 26 w/w %; [ProGel-SIM] = 15 w/v %) treatment weekly to the periodontal pocket of a rat PD model (Figure 1E) for 3 weeks. As shown in Figure 4A, the distance between the maxillary molar (M1−M2) cementoenamel junction (CEJ) and the alveolar bone crest (ABC) in rats treated with ProGel-SIM appears to be shorter than those treated with SMA and Saline. The quantitative analysis of the CEJ-ABC measurement was presented in Figure 4G, where the average CEJ-ABC measurement for rats in the ProGel-SIM group was found to be significantly lower than those in SMA (0.63 vs 0.90 mm) and Saline group (0.63 vs 0.92 mm). When compared to the Healthy control, the ProGel-SIM-treated rats showed a significantly higher CEJ-ABC value (0.63 vs 0.39 mm). In addition to CEJ-ABC distance, quantitative analyses for other parameters reflecting bone quality were performed (Figure 4C−F). Alveolar bone quality in rats treated with ProGel-SIM was also improved with significantly better bone volume (BV, 0.34 mm^3), bone volume fraction (BV/TV, 11.63%), trabecular thickness (Tb.Th, 0.10 mm), and trabecular separation (Tb.Sp, 0.48 mm) when compared to those treated with SMA (BV: 0.20 mm^3, BV/TV: 6.92%, Tb.Th: 0.09 mm, and Tb.Sp: 0.57 mm) and Saline (BV: 0.17 mm^3, BV/TV: 5.35%, Tb.Th: 0.08 mm, and Tb.Sp: 0.55 mm). Nevertheless, the healthy rats still had the best alveolar bone quality (BV: 0.44 mm^3, BV/TV: 16.57%, Tb.Th: 0.12 mm; Tb.Sp: 0.40 mm). Importantly, the 3D representation of alveolar bone from each group (Figure 4B) showed that the bone loss associated with ligature-induced PD was not limited to the area between the first (M1) and second molar (M2) but was much more extensive. The rats treated with ProGel-SIM had much healthier periodontal bone quality when compared to the SMA and Saline groups. Given the capability of SIM to upregulate BMP-2, a potent osteogenic factor that promotes bone formation,[15,25] it is of great interest to understand if the observed capacity of ProGel-SIM in improving periodontal bone quality of the PD rat model was mediated through the BMP-2 pathway. As the IHC results show in Figure 4H and I, the ProGel-SIM treated rats were observed with higher levels of BMP-2 expression than those found in the SMA-treated rats, confirming ProGel-SIM's mechanism of action in restoring periodontal bone quality is at least in part attributed to local BMP-2 upregulation.

Periodontal Application of ProGel-SIM Significantly Reduced the Inflammatory Cell Infiltration and Cytokines Release. The presence of microbiomes around ligature placement stimulates inflammatory responses, resulting in the recruitment of immune cells such as polymorphonuclear leukocytes (PMN) and specific T lymphocyte subsets (i.e., T_h17 cells). Their interaction with the microbiome would lead to the first wave of cytokine secretion, including the interleukin-1 (IL-1) family, the interleukin-6 (IL-6) family, and tumor necrosis factor (TNF), culminating in periodontal tissue damages.[45] As a thermoresponsive polymeric prodrug of SIM, periodontal instillation of ProGel-SIM provides a mechanism for sustained local activation and release of the anti-inflammatory SIM at PD pathology. To assess ProGel-SIM's local anti-inflammation capacity, the HE-stained palate sections were scored for PMN and T lymphocyte infiltration by a pathologist (SML) who was blinded to the experimental grouping (Figure 5A). IHC was used to assess the levels of IL-1β and TNF-α (Figure 5B,C). As shown in Figure 6A, the

https://doi.org/10.1021/acs.molpharmaceut.3c00508
Mol. Pharmaceutics 2023, 20, 5631−5645

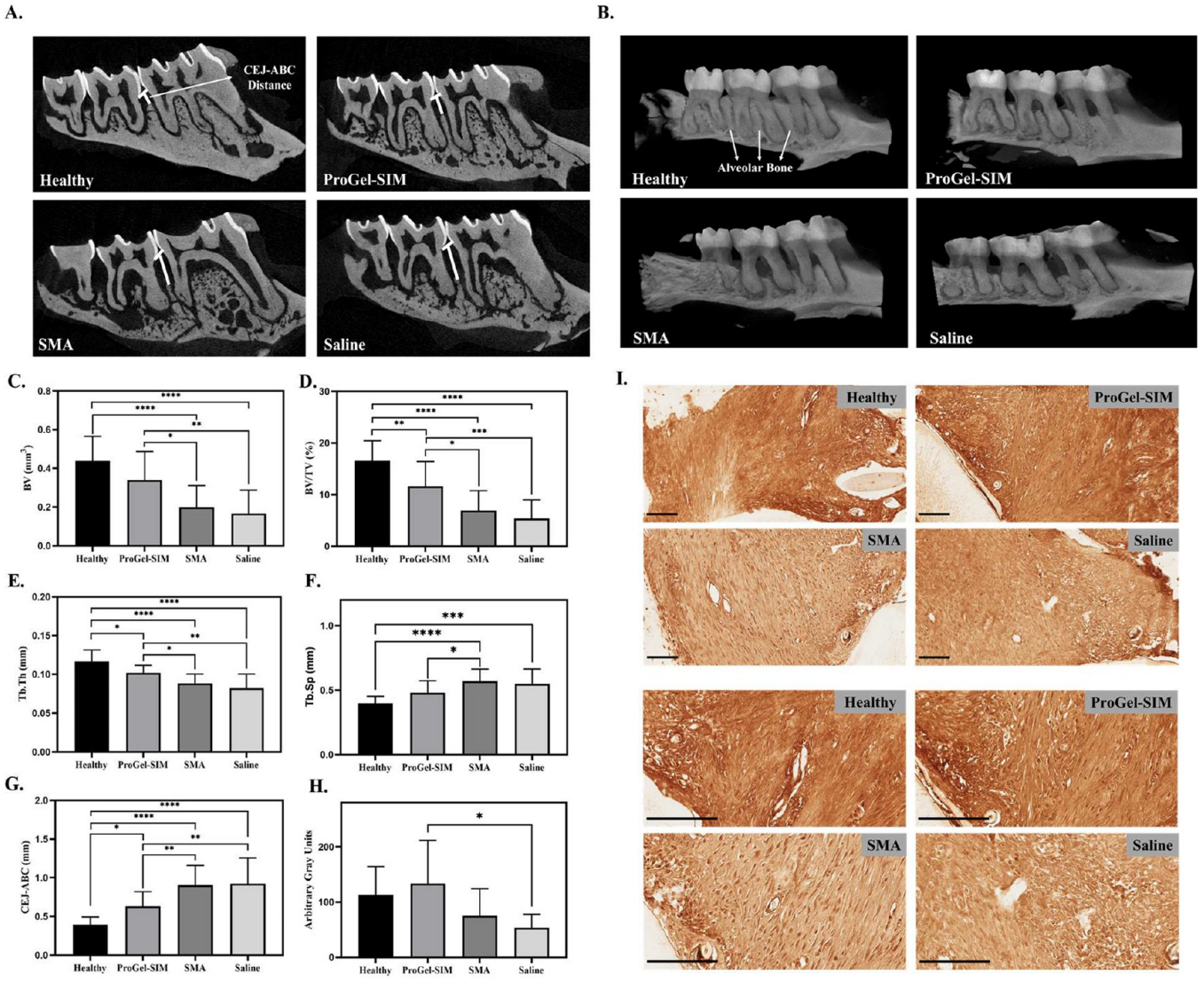

Figure 4. *In vivo* evaluation of alveolar bone quality in four treatment groups. Representative (A) 2D and (B) 3D μ-CT sagittal images of rats in the Healthy group (positive control group), ProGel-SIM group, Simvastatin acid (SMA) group, and Saline group (negative control group). The white vertical lines indicate the distance from the cementoenamel junction to the alveolar bone crest (CEJ-ABC distance). μ-CT morphometric analysis showed the quantitative parameters. Quantification of (C) Bone volume (BV), (D) Bone volume fraction (BV/TV), (E) Trabecular thickness (Tb.Th), and (F) Trabecular separation (Tb.Sp) for alveolar bone after 3 weeks of treatment (n = 16). (G) Measurement of linear distance between CEJ and ABC (n = 16). (H) Semiquantification of the BMP-2 expression in the connective tissue between M1 and M2 (n = 8). (I) Representative images of IHC staining for assessing the expression level of BMP-2. The images were captured under 200× (upper four panels) and 400× (lower four panels) magnification. Scale bar = 100 μm. Data are expressed as mean ± SD * P < 0.05; ** P < 0.01; *** P < 0.001; **** P < 0.0001 (one-way ANOVA with Tukey's *post hoc* test for multiple comparisons).

scores of PMN for rats in ProGel-SIM and Healthy groups were significantly lower than those in rats treated with SMA and Saline. The level of lymphocyte infiltration (Figure 6B) was significantly higher in the Saline group when compared to the Healthy control but was not significantly different from the ProGel-SIM and SMA-treated rats. Though no significant difference was observed, the average lymphocytes score for ProGel-SIM and SMA-treated rats were lower than that of the Saline group. These results suggest that ProGel-SIM treatment was more effective in inhibiting inflammatory cell infiltration than SMA. The semiquantitative IHC analysis suggests that the expression levels of IL-1β in Healthy and ProGel-SIM-treated rats were significantly lower than those in rats treated with SMA and saline (Figure 6C). No significant difference in TNF-α level was observed among all tested groups, but the Healthy and ProGel-SIM-treated rats exhibited a trend of lower TNF-α expression than those in rats treated with SMA and Saline (Figure 6D). Together, these results confirmed ProGel-SIM's superior capacity in dampening the inflammation of the rats' periodontium when compared with SMA and Saline groups. The dampened inflammatory condition also explains the better bone quality found in the ProGel-SIM-treated rats.

Local Application of SIM Showed No Hepatic Adverse Effect. Though overall being considered a very safe medication, statins have been recognized for their potential hepatotoxicity.[46] Though not fully established, it has been speculated that statins may affect membrane lipid composition, and increase permeability, resulting in the leakage of the liver enzymes.[47] Clinically, the screening of liver functions can be performed to avoid the prescription of statins

https://doi.org/10.1021/acs.molpharmaceut.3c00508
Mol. Pharmaceutics 2023, 20, 5631−5645

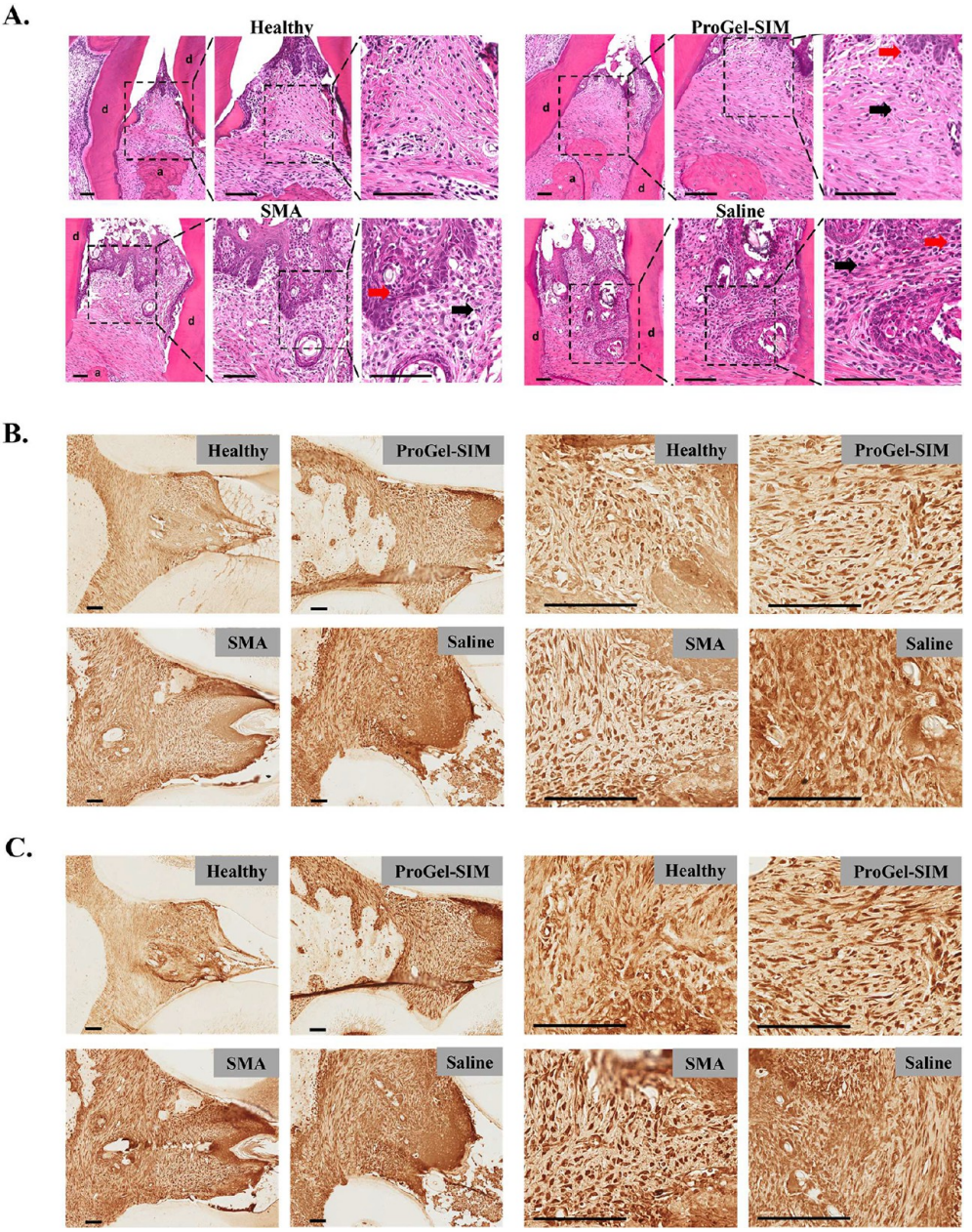

Figure 5. Histological assessment of the inflammatory status in connective tissue between M1 and M2. (A) Representative images of HE staining for assessing the infiltration of polymorphonuclear leukocytes (Red arrow) and lymphocytes (Black arrow) in connective tissue between M1 and M2. The images were captured under 100×, 200×, and 400× magnification. The alveolar bone (a) and dentin (d) were marked in the images with 100× magnification. Representative images of IHC staining for assessing the expression levels of (B) IL-1β and (C) TNF-α in connective tissue between M1 and M2. The images were captured under 100× (left) and 400× (right) magnification. Scale bar = 100 μm.

to patients who may already have compromised liver functions.[48] To understand if ProGel-SIM treatment may negatively affect the liver, we evaluated the levels of serum alanine aminotransferase (ALT), albumin (ALB), and alkaline phosphatase (ALP). The elevation of serum ALT is most widely reported to be associated with statins' hepatoxicity.[48,49] As shown in Figure 7, ProGel-SIM and SMA-treated rats shared similar ALT, ALB, and ALP levels as the Healthy rats.

DISCUSSION

3-Hydroxy-3-methyl glutaryl coenzyme A (HMG-CoA) reductase plays a critical role in converting HMG-CoA into mevalonate, which is a rate-limiting step in the synthesis of cholesterol. As a potent HMG-CoA inhibitor, simvastatin (SIM) has been widely used to treat hyperlipidemia,[12] hypercholesterolemia,[44] and atherosclerosis.[14] In addition to these well-established clinical applications, many studies have validated the potential of repurposing SIM as a novel treatment for PD. The rationale behind the proposed repurposing is attributed to SIM's anti-inflammatory and bone anabolic capabilities.[50−53] Previously, to overcome SIM's poor water-solubility and the lack of osteotropicity, we have developed several formulations of SIM (e.g., SIM-PPi[35] and SIM-loaded PF127[54]) for the treatment of experimental PD in rats. The conjugation of SIM to pyrophosphate (PPi) improved its water-solubility and introduced osteotropicity. The local SIM dosing level was limited, however, by the availability of PPi

https://doi.org/10.1021/acs.molpharmaceut.3c00508
Mol. Pharmaceutics 2023, 20, 5631−5645

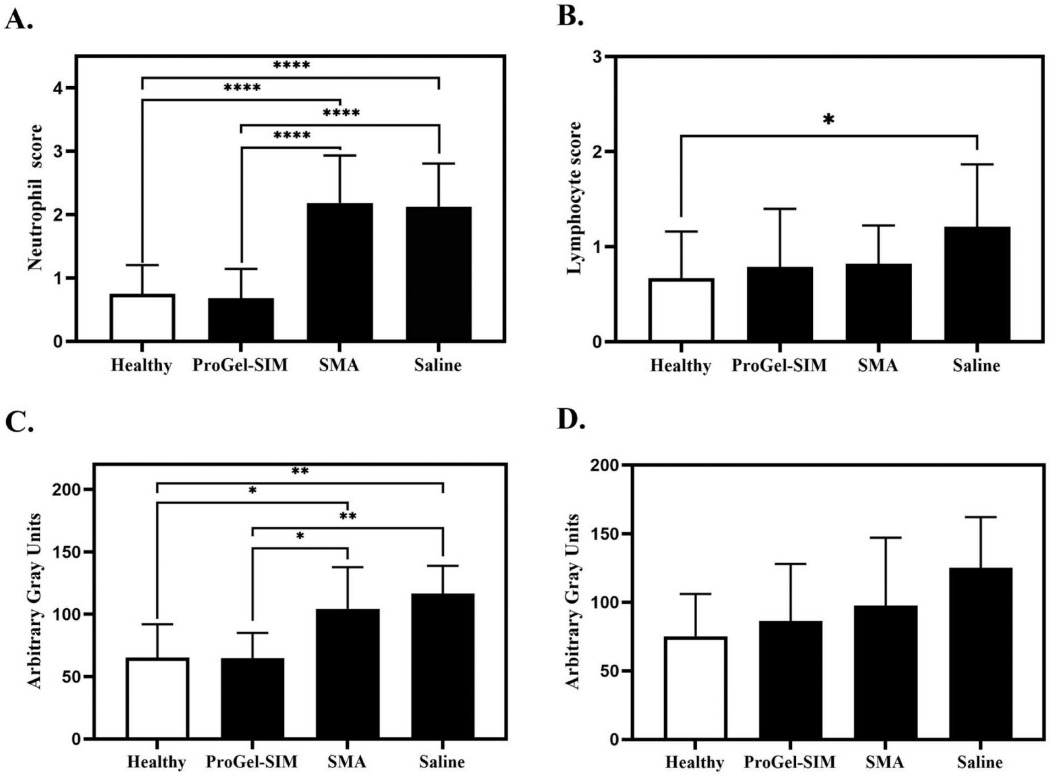

Figure 6. Semiquantitative analysis of the immune cells' infiltration and cytokines' secretion. The pathological scores for infiltration of (A) PMNs (n = 12) and (B) lymphocytes (n = 12) were assessed by a pathologist, and the expression of (C) IL-1β (n = 8) and (D) TNF-α (n = 8) was semiquantified by ImageJ. Data are expressed as mean ± SD * P < 0.05; ** P < 0.01; **** P < 0.0001 (For pathological scoring, the Mann−Whitney U test was used. For comparing the cytokines' expression level, one-way ANOVA with Tukey's *post hoc* test for multiple comparisons was used).

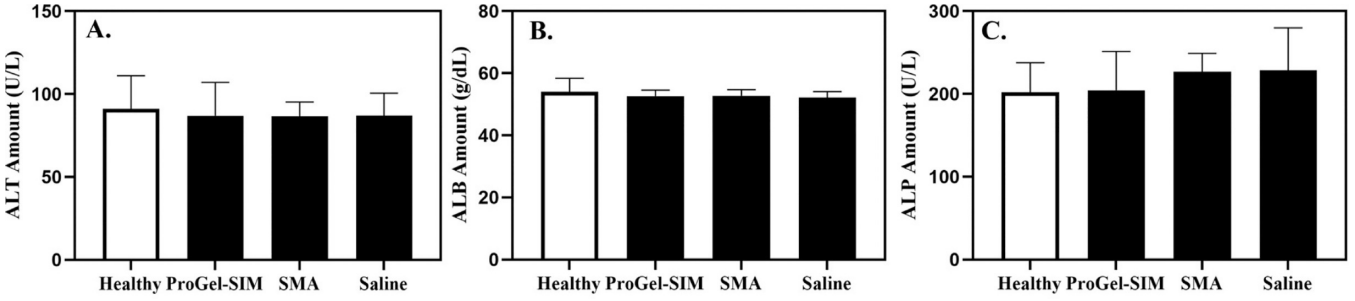

Figure 7. Impact of local ProGel-SIM treatment on liver functions. The (A) alanine aminotransferase (ALT), (B) albumin (ALB), and (C) alkaline phosphatase (ALP) in the serum were analyzed and compared with different treatment groups (n = 8). There was no significant difference between the Healthy rats and the rats treated with ProGel-SIM and SMA, indicating that neither ProGel-SIM nor SMA would lead to hepatoxicity. Data are expressed as mean ± SD.

binding sites in the periodontal pocket. For the SIM-loaded thermoresponsive PPi-functionalized F127 hydrogel system, the local SIM-dosing level was also limited by the F127 encapsulation capacity. Building upon these previous experiences, we developed and tested a novel thermoresponsive SIM prodrug (ProGel-SIM) in this study. The thermoresponsive property of the ProGel-SIM, which was confirmed by the tube-tilting method and rheology study, allows the *in vivo* hydrogel formation and physical entrapment of the polymeric prodrug of SIM in the periodontal pocket. Since SIM was chemically conjugated to the HPMA copolymer, its activation was more tightly regulated by the local pathophysiology. Given the 22−26 w/w % SIM content in the ProGel-SIM tested in this study, it also presented a much higher SIM loading capacity than the PF127 system.

The thermoresponsive property of ProGel-SIM offers a simple strategy for sustained local SIM delivery. To understand the inner structure change of ProGel-SIM at different temperatures, SAXS analysis was performed. Based on the outcome of this study and the chemical structures of the ProGel-SIM, we speculated the following as the potential mechanism for ProGel-SIM's thermoresponsive phase transition. Thermoresponsive polymeric prodrugs (ProGel) systems,[31] such as ProGel-SIM, consist of the hydrophobic element (e.g., SIM), hydrophilic element (e.g., HPMA copolymer), and water in which ProGel-SIM is dissolved. The observed alternation of the R_g accompanying the

https://doi.org/10.1021/acs.molpharmaceut.3c00508
Mol. Pharmaceutics 2023, 20, 5631−5645

thermoresponsive gelation may reflect the increase in SIM aggregation and formation of physical cross-links with the increased energy input (temperature increased from 5 to 35 °C). When additional energy was introduced (temperature raised to ∼45 °C), the hydrophobic SIM molecules would further aggregate, forcing the dehydration and partial collapse of the hydrophilic HPMA copolymer chains and the macroscopic observation of water being expelled from the hydrogel (i.e., syneresis). Such temperature-dependent change of R_g is not a unique feature of ProGel systems but shared by other thermoresponsive hydrogel systems such as poly(*N*-isopropylacrylamide) (PNIPAM).[55,56]

The ProGel-SIM used for *in vivo* study had an M_w of ∼8.5 kDa, which is much lower than the kidney glomerular filtration threshold (<45 kDa) for HPMA copolymers.[57] It predicates swift renal clearance if it is absorbed locally and enters circulation. For the ProGel-SIM that escapes the periodontal pocket and migrates into the GI tract, the polymeric prodrug of SIM will likely be activated by the acidity of the gastric environment, followed by the intestinal SIM absorption and the excretion of the HPMA copolymer carrier. Based on the thermoresponsive phase transition diagram of ProGel-SIM, SIM content and the prodrug concentration directly regulate the gelation and syneresis temperatures of ProGel-SIM. These formulation parameters also control the ProGel-SIM erosion/dissolution kinetics. In addition to erosion kinetics, cellular uptake of the drug is another important aspect of therapeutic efficacy. Different from the small molecules, which passively diffuse to the cytosol, the nanometer-sized polymeric prodrug of SIM enters cells via the endocytic pathway. In PD pathology, there were many mononuclear phagocytes populated at the site of inflammation.[45] When preferentially sequestered by these highly phagocytic cells, ProGel-SIM will be activated to release SIM and exert its anti-inflammation activity, specifically within these pathogenic cells.

While SIM has been used extensively and safely as an oral medication for decades, it can induce myopathy and hepatitis if given at high doses.[58,59] Local application of SIM at high doses may also have negative impacts on oral health.[60] Given these potential safety risks, we performed cell viability studies using two cell lines that are relevant to periodontal pathophysiology. The *in vitro* cell culture results from mouse macrophages (RAW 264.7), and osteoblasts (3T3-L1) suggested that ProGel-SIM is safe and may significantly reduce the cytotoxicity of SIM at high concentrations and mitigate the risk of local tissue damages that may be elicited by high doses of SIM. We attribute this observation to the polymeric prodrug nature of ProGel-SIM and the utility of HPMA copolymers, which are known to have excellent biocompatible.[61] To further confirm the *in vivo* safety profile of ProGel-SIM, we evaluated the liver functions of the rats by assessing the levels of serum ALT, ALB, and ALP. We found that their levels were not significantly altered by the treatment of ProGel-SIM and SMA, suggesting that the local application of the SIM formulations would avoid systemic complications. Interestingly, ALP can also be released by PMN and be significantly elevated due to PD.[62] Therefore, it has been used as a diagnostic marker for periodontal disease.[63] Even though no significant difference in ALP was observed among all four tested groups, the average ALP levels in ProGel-SIM-treated and Healthy rats were lower than those of the rats in the other two groups. This observation can be further investigated as additional evidence for ProGel-SIM's superior efficacy in ameliorating periodontal inflammation.

The therapeutic efficacy of ProGel-SIM was evaluated in a well-established experimental PD rat model.[36] Once the PD pathology was established, the ProGel-SIM solution was injected via a 31-G syringe into the periodontal pocket, where it formed a hydrogel instantly. The prodrug hydrogel would gradually dissolve and permeate the periodontal tissue, where tissue acidity[40] and the presence of leukocyte esterase[64] would cause the cleavage of ester bonds in ProGel-SIM to release SIM and SMA (an active form of SIM). It was shown that the alveolar bone quality and the inflammatory condition in the connective tissue of the rats treated with ProGel-SIM were significantly improved when compared to the rats treated with SMA or saline, suggesting that the local delivery of SIM using the ProGel-SIM system is very effective in preserving/regenerating periodontal bone and in mitigating local inflammation associated with PD pathology. After evaluating the expression level of BMP-2, which is known to mediate SIM's bone anabolic activities, we found that the ProGel-SIM treated rats had higher expression of BMP-2 when compared to SMA and Saline groups, suggesting that the better performance of the ProGel-SIM in stimulating bone regeneration is through increasing the BMP-2 expression. Nevertheless, the ProGel-SIM treatment did not fully restore the periodontal bone quality comparable to the level of Healthy rats and did not completely eradicate the soft tissue inflammation, which may be attributed to the chronic presence of periodontal bacterial infection. In clinics, scaling and root planing must be performed to eliminate biofilms before the application of any medications. Therefore, we may consider including these procedures before the application of ProGel-SIM. Even though SIM was known for its moderate antimicrobial capability, it appears to be insufficient to change the local infection status. Therefore, the incorporation of antibiotics in the ProGel-SIM formulation, either through physical encapsulation or in combination with a ProGel-antimicrobial formulation, should be explored in the future development of more effective therapies for PD and associated pathologies.

CONCLUSIONS

ProGel-SIM, a novel thermoresponsive polymeric prodrug of simvastatin (SIM), was designed, synthesized, and characterized in this study. The observed thermoresponsive properties of ProGel-SIM were found to be feasible for *in vivo* applications as a potential treatment for symptoms associated with periodontitis (PD). Detailed SAXS analyses confirmed the driving force of ProGel-SIM's thermoresponsive properties could be attributed to the temperature-dependent self-assembly and aggregation of the hydrophobic SIM within the water-soluble polymeric prodrug. *In vitro* and *in vivo* assessments of ProGel-SIM confirmed its excellent safety and therapeutic potential as a novel drug candidate for the clinical management of periodontitis. Further investigations, including the combination with antimicrobials, may be necessary to develop it into a highly effective treatment for PD.

ASSOCIATED CONTENT

Supporting Information

The Supporting Information is available free of charge at https://pubs.acs.org/doi/10.1021/acs.molpharmaceut.3c00508.

https://doi.org/10.1021/acs.molpharmaceut.3c00508
Mol. Pharmaceutics 2023, 20, 5631−5645

NMR spectra of ProGel-SIM and compounds **1**, **2**, and **3** (PDF)

AUTHOR INFORMATION

Corresponding Author

Dong Wang − *Department of Pharmaceutical Sciences, College of Pharmacy, University of Nebraska Medical Center, Omaha, Nebraska 68198, United States;* orcid.org/0000-0002-8340-2763; Phone: 402-559-1995; Email: dwang@unmc.edu; Fax: 402-559-9543

Authors

Xiaoke Xu − *Department of Pharmaceutical Sciences, College of Pharmacy, University of Nebraska Medical Center, Omaha, Nebraska 68198, United States*

Zhenshan Jia − *Department of Pharmaceutical Sciences, College of Pharmacy, University of Nebraska Medical Center, Omaha, Nebraska 68198, United States*

Ningrong Chen − *Department of Pharmaceutical Sciences, College of Pharmacy, University of Nebraska Medical Center, Omaha, Nebraska 68198, United States*

Subodh M. Lele − *Department of Pathology and Microbiology, College of Medicine, University of Nebraska Medical Center, Omaha, Nebraska 68198, United States*

Shabnam Arash − *Department of Pharmaceutical Sciences, College of Pharmacy, University of Nebraska Medical Center, Omaha, Nebraska 68198, United States*

Richard A. Reinhardt − *Department of Surgical Specialties, College of Dentistry, University of Nebraska Medical Center, Omaha, Nebraska 68198, United States*

Amy C. Killeen − *Department of Surgical Specialties, College of Dentistry, University of Nebraska Medical Center, Omaha, Nebraska 68198, United States*

Complete contact information is available at: https://pubs.acs.org/10.1021/acs.molpharmaceut.3c00508

Author Contributions

[⊥]XX and ZSJ contributed equally to this work.

Notes

The authors declare the following competing financial interest(s): ZSJ and DW are co-inventors of the ProGel technology described in this manuscript. A PCT patent application has been filed to protect the technology. DW is a co-founder of Ensign Pharmaceutical, which has licensed the ProGel technology for further development and clinical translation.

ACKNOWLEDGMENTS

This study was supported, in part, by the National Institute of Arthritis and Musculoskeletal and Skin Diseases of the United States National Institutes of Health (R01 AR082148) and UNMC College of Pharmacy. The content is solely the authors' responsibility and does not necessarily represent the official views of the National Institutes of Health.

REFERENCES

(1) Kwon, T.; Lamster, I. B.; Levin, L. Current Concepts in the Management of Periodontitis. *International Dental Journal* **2021**, *71* (6), 462−476.

(2) Hajishengallis, G. Immunomicrobial pathogenesis of periodontitis: keystones, pathobionts, and host response. *Trends Immunol* **2014**, *35* (1), 3−11.

(3) Pihlstrom, B. L.; Michalowicz, B. S.; Johnson, N. W. Periodontal diseases. *Lancet* **2005**, *366* (9499), 1809−1820.

(4) Hajishengallis, G.; Darveau, R. P.; Curtis, M. A. The keystone-pathogen hypothesis. *Nat. Rev. Microbiol* **2012**, *10* (10), 717−725.

(5) Tonetti, M. S.; Jepsen, S.; Jin, L.; Otomo-Corgel, J. Impact of the global burden of periodontal diseases on health, nutrition and wellbeing of mankind: A call for global action. *J. Clin Periodontol* **2017**, *44* (5), 456−462.

(6) Romandini, M.; Laforí, A.; Romandini, P.; Baima, G.; Cordaro, M. Periodontitis and platelet count: A new potential link with cardiovascular and other systemic inflammatory diseases. *J. Clin Periodontol* **2018**, *45* (11), 1299−1310.

(7) Yoon, A. J.; Cheng, B.; Philipone, E.; Turner, R.; Lamster, I. B. Inflammatory biomarkers in saliva: assessing the strength of association of diabetes mellitus and periodontal status with the oral inflammatory burden. *J. Clin Periodontol* **2012**, *39* (5), 434−440.

(8) de Pablo, P.; Chapple, I. L. C.; Buckley, C. D.; Dietrich, T. Periodontitis in systemic rheumatic diseases. *Nat. Rev. Rheumatol* **2009**, *5* (4), 218−224.

(9) Apatzidou, D. A.; Kinane, D. F. Nonsurgical Mechanical Treatment Strategies for Periodontal Disease. *Dent Clin North Am.* **2010**, *54* (1), 1−12.

(10) Dommisch, H.; Walter, C.; Dannewitz, B.; Eickholz, P. Resective surgery for the treatment of furcation involvement: A systematic review. *J. Clin Periodontol* **2020**, *47*, 375−391.

(11) Prakasam, A.; Elavarasu, S. S.; Natarajan, R. K. Antibiotics in the management of aggressive periodontitis. *J. Pharm. Bioallied Sci.* **2012**, *4*, S252−255.

(12) Mahboobian, M. M.; Dadashzadeh, S.; Rezaei, M.; Mohammadi, M.; Bolourchian, N. Simvastatin in ternary solid dispersion formulations: Improved In vitro dissolution and anti-hyperlipidemia efficiency. *J. Drug Deliv Sci. Tech* **2022**, *74*, No. 103571.

(13) Taylor, F.; Huffman, M. D.; Macedo, A. F.; Moore, T. H. M.; Burke, M.; Smith, G. D.; Ward, K.; Ebrahim, S.; et al. Statins for the primary prevention of cardiovascular disease. *Cochrane Database Syst. Rev.* **2021**, *2013* (1), No. CD004816.

(14) Ridker, P. M.; Pradhan, A.; MacFadyen, J. G.; Libby, P.; Glynn, R. J. Cardiovascular benefits and diabetes risks of statin therapy in primary prevention: an analysis from the JUPITER trial. *Lancet* **2012**, *380* (9841), 565−571.

(15) Mundy, G.; Garrett, R.; Harris, S.; Chan, J.; Chen, D.; Rossini, G.; Boyce, B.; Zhao, M.; Gutierrez, G. Stimulation of Bone Formation in Vitro and in Rodents by Statins. *Science* **1999**, *286* (5446), 1946−1949.

(16) Thylin, M. R.; McConnell, J. C.; Schmid, M. J.; Reckling, R. R.; Ojha, J.; Bhattacharyya, I.; Marx, D. B.; Reinhardt, R. A. Effects of Simvastatin Gels on Murine Calvarial Bone. *J. Periodontol* **2002**, *73* (10), 1141−1148.

(17) Kim, C. H.; Choi, K. S.; Lee, I. K.; Park, J. U.; Pyo, S. W. The effect of simvastatin on osteogenic differentiation of human buccal fat pad-derived stem cells. *Tissue Eng. Regen Med.* **2009**, *6* (1), 2−8.

(18) Chuengsamarn, S.; Rattanamongkoulgul, S.; Suwanwalaikorn, S.; Wattanasirichaigoon, S.; Kaufman, L. Effects of statins vs. non-statin lipid-lowering therapy on bone formation and bone mineral density biomarkers in patients with hyperlipidemia. *Bone* **2010**, *46* (4), 1011−1015.

(19) Masuzaki, T.; Ayukawa, Y.; Moriyama, Y.; Jinno, Y.; Atsuta, I.; Ogino, Y.; Koyano, K. The effect of a single remote injection of statin-impregnated poly (lactic-co-glycolic acid) microspheres on osteogenesis around titanium implants in rat tibia. *Biomaterials* **2010**, *31* (12), 3327−3334.

(20) Ifergan, I.; Wosik, K.; Cayrol, R.; Kébir, H.; Auger, C.; Bernard, M.; Bouthillier, A.; Moumdjian, R.; Duquette, P.; Prat, A. Statins reduce human blood−brain barrier permeability and restrict leukocyte migration: relevance to multiple sclerosis. *Ann. Neurol.* **2006**, *60* (1), 45−55.

(21) Lin, R.; Liu, J.; Peng, N.; Gan, W.; Wang, W.; Han, C.; Ding, C. Lovastatin reduces apoptosis and downregulates the CD40 expression

induced by TNF-α in cerebral vascular endothelial cells. *Curr. Neurovascular Res.* **2006**, *3* (1), 41−47.
(22) Eccles, K. A.; Sowden, H.; Porter, K. E.; Parkin, S. M.; Homer-Vanniasinkam, S.; Graham, A. M. Simvastatin alters human endothelial cell adhesion molecule expression and inhibits leukocyte adhesion under flow. *Atherosclerosis* **2008**, *200* (1), 69−79.
(23) Liang, Y.-J.; Shyu, K.-G.; Wang, B.-W.; Lai, L.-P. Simvastatin inhibits C-reactive protein-induced pro-inflammatory changes in endothelial cells by decreasing mevalonate pathway products. *Cardiology* **2008**, *110* (3), 182−190.
(24) Sugiyama, M.; Kodama, T.; Konishi, K.; Abe, K.; Asami, S.; Oikawa, S. Compactin and simvastatin, but not pravastatin, induce bone morphogenetic protein-2 in human osteosarcoma cells. *Biochem. Biophys. Res. Commun.* **2000**, *271* (3), 688−692.
(25) Maeda, T.; Matsunuma, A.; Kurahashi, I.; Yanagawa, T.; Yoshida, H.; Horiuchi, N. Induction of osteoblast differentiation indices by statins in MC3T3-E1 cells. *J. Cell Biochem* **2004**, *92* (3), 458−471.
(26) Emani, S.; Gunjiganur, G. V.; Mehta, D. S. Determination of the antibacterial activity of simvastatin against periodontal pathogens, Porphyromonas gingivalis and Aggregatibacter actinomycetemcomitans: An in vitro study. *Contemp Clin Dent* **2014**, *5* (3), 377−382.
(27) Sakoda, K.; Yamamoto, M.; Negishi, Y.; Liao, J. K.; Node, K.; Izumi, Y. Simvastatin Decreases IL-6 and IL-8 Production in Epithelial Cells. *J. Dent Res.* **2006**, *85* (6), 520−523.
(28) Ismail, F. A. Design and in vitro evaluation of polymeric formulae of simvastatin for local bone induction. *Drug Dev. Ind. Pharm.* **2006**, *32* (10), 1199−1206.
(29) Cunha-Cruz, J.; Saver, B.; Maupome, G.; Hujoel, P. P. Statin Use and Tooth Loss in Chronic Periodontitis Patients. *J. Periodontol* **2006**, *77* (6), 1061−1066.
(30) Kaminsky, Y.; Kosenko, E. Molecular mechanisms of toxicity of simvastatin, widely used cholesterol-lowering drug. A review. *Open Med.* **2010**, *5* (3), 269−279.
(31) Zhao, G.; Ren, R.; Wei, X.; Jia, Z.; Chen, N.; Sun, Y.; Zhao, Z.; Lele, S. M.; Zhong, H. A.; Goldring, M. B.; Goldring, S. R.; Wang, D. Thermoresponsive polymeric dexamethasone prodrug for arthritis pain. *J. Controlled Release* **2021**, *339*, 484−497.
(32) Chung, Y. M.; Simmons, K. L.; Gutowska, A.; Jeong, B. Sol-gel transition temperature of PLGA-g-PEG aqueous solutions. *Biomacromolecules* **2002**, *3* (3), 511−516.
(33) Manalastas-Cantos, K.; Konarev, P. V.; Hajizadeh, R.; Kikhney, A. G.; Petoukhov, M. V.; Molodenskiy, D. S.; Panjkovich, A.; Mertens, H. D. T.; Gruzinov, A.; Borges, C.; Jeffries, C. M.; Svergun, D. I.; Franke, D. ATSAS 3.0: expanded functionality and new tools for small-angle scattering data analysis. *J. Appl. Crystallogr.* **2021**, *54* (1), 343−355.
(34) Yoshinari, M.; Matsuzaka, K.; Hashimoto, S.; Ishihara, K.; Inoue, T.; Oda, Y.; Ide, T.; Tanaka, T. Controlled release of simvastatin acid using cyclodextrin inclusion system. *Dent Mater. J.* **2007**, *26* (3), 451−456.
(35) Wang, X.; Jia, Z.; Almoshari, Y.; Lele, S. M.; Reinhardt, R. A.; Wang, D. Local Application of Pyrophosphorylated Simvastatin Prevents Experimental Periodontitis. *Pharm. Res.* **2018**, *35* (8), No. 164.
(36) Marchesan, J.; Girnary, M. S.; Jing, L.; Miao, M. Z.; Zhang, S.; Sun, L.; Morelli, T.; Schoenfisch, M. H.; Inohara, N.; Offenbacher, S.; Jiao, Y. An experimental murine model to study periodontitis. *Nat. Protoc* **2018**, *13* (10), 2247−2267.
(37) Crowe, A. R.; Yue, W. Semi-quantitative Determination of Protein Expression using Immunohistochemistry Staining and Analysis: An Integrated Protocol. *Bio Protoc* **2019**, *9* (24), No. e3465.
(38) Larsen, E. M.; Johnson, R. J. Microbial esterases and ester prodrugs: An unlikely marriage for combating antibiotic resistance. *Drug Dev Res.* **2019**, *80* (1), 33−47.
(39) Vprb, R. R.; Thamaraiselvan, M. Role of Salivary PH on the Prevalence of Periodontal Disease: A Cross Sectional Pilot Study. *J. Med. Dent Sci.* **2020**, *8*, 423−427.
(40) Lăzureanu, P. C.; Popescu, F.; Tudor, A.; Stef, L.; Negru, A. G.; Mihăilă, R. Saliva pH and Flow Rate in Patients with Periodontal Disease and Associated Cardiovascular Disease. *Med. Sci. Monit* **2021**, *27*, No. e931362.
(41) Kim, C.; Jarumaneeroj, C.; Rungswang, W.; Jin, K. S.; Ree, M. A comprehensive small angle X-ray scattering analysis on morphological structure of semicrystalline linear polymer in bulk state. *Polymer* **2022**, *243*, No. 124610.
(42) Kikhney, A. G.; Svergun, D. I. A practical guide to small angle X-ray scattering (SAXS) of flexible and intrinsically disordered proteins. *FEBS Lett.* **2015**, *589*, 2570−2577.
(43) Rihova, B.; Kovár, M. Immunogenicity and immunomodulatory properties of HPMA-based polymers. *Adv. Drug Deliv Rev.* **2010**, *62*, 184−191.
(44) Gao, X.; Zhou, J.; Bian, Y.; Huang, S.; Zhang, D. Simvastatin intervention mitigates hypercholesterolemia-induced alveolar bone resorption in rats. *Exp Ther Med.* **2021**, *21* (6), No. 628.
(45) Pan, W.; Wang, Q.; Chen, Q. The cytokine network involved in the host immune response to periodontitis. *Int. J. Oral Sci.* **2019**, *11* (3), No. 30.
(46) Law, M.; Rudnicka, A. R. Statin safety: a systematic review. *J. Am. Coll Cardiol* **2006**, *97* (8), S52−S60.
(47) Gluba-Brzozka, A.; Franczyk, B.; Toth, P. P.; Rysz, J.; Banach, M. Molecular mechanisms of statin intolerance. *Arch Med. Sci.* **2016**, *12* (3), 645−658.
(48) Thapar, M.; Russo, M. W.; Bonkovsky, H. L. Statins and liver injury. *Gastroenterol Hepatol (N Y)* **2013**, *9* (9), 605−606.
(49) Armitage, J.; Bowman, L.; Collins, R.; Parish, S.; Tobert, J. Effects of simvastatin 40 mg daily on muscle and liver adverse effects in a 5-year randomized placebo-controlled trial in 20,536 high-risk people. *BMC Clin Pharmacol* **2009**, *9*, 6.
(50) Xu, L.; Sun, X.; Zhu, G.; Mao, J.; Baban, B.; Qin, X. Local delivery of simvastatin maintains tooth anchorage during mechanical tooth moving via anti-inflammation property and AMPK/MAPK/NF-kB inhibition. *J. Cell Mol. Med.* **2021**, *25* (1), 333−344.
(51) Yan, J.; Liu, A.; Fan, H.; Qiao, L.; Wu, J.; Shen, M.; Lai, X.; Huang, J. Simvastatin Improves Behavioral Disorders and Hippocampal Inflammatory Reaction by NMDA-Mediated Anti-inflammatory Function in MPTP-Treated Mice. *Cell Mol. Neurobiol* **2020**, *40* (7), 1155−1164.
(52) Zamani, M.; Shirinzadeh, A.; Aghajanzadeh, M.; Andalib, S.; Danafar, H. In vivo study of mPEG−PCL as a nanocarriers for anti-inflammatory drug delivery of simvastatin. *Pharm. Dev Technol.* **2019**, *24* (6), 663−670.
(53) Özeç, I.; Kiliç, E.; Gümüş, C.; Göze, F. Effect of Local Simvastatin Application on Mandibular Defects. *J. Craniofacial Surg* **2007**, *18* (3), 546−550.
(54) Chen, N.; Ren, R.; Wei, X.; Mukundan, R.; Li, G.; Xu, X.; Zhao, G.; Zhao, Z.; Lele, S. M.; Reinhardt, R. A.; Wang, D. Thermoresponsive Hydrogel-Based Local Delivery of Simvastatin for the Treatment of Periodontitis. *Mol. Pharmaceutics* **2021**, *18* (5), 1992−2003.
(55) Wang, X.; Qiu, X.; Wu, C. Comparison of the Coil-to-Globule and the Globule-to-Coil Transitions of a Single Poly(N-isopropylacrylamide) Homopolymer Chain in Water. *Macromolecules* **1998**, *31* (9), 2972−2976.
(56) Wang, X.; Wu, C. Light-Scattering Study of Coil-to-Globule Transition of a Poly(*N*-isopropylacrylamide) Chain in Deuterated Water. *Macromolecules* **1999**, *32* (13), 4299−4301.
(57) Chytil, P.; Kostka, L.; Etrych, T. HPMA Copolymer-Based Nanomedicines in Controlled Drug Delivery. *J. Pers Med.* **2021**, *11* (2), 115.
(58) Yang, H. J.; Choi, M.-J.; Wen, H.; Kwon, H. N.; Jung, K. H.; Hong, S.-W.; Kim, J. M.; Hong, S.-S.; Park, S. An effective assessment of simvastatin-induced toxicity with NMR-based metabonomics approach. *PLoS One* **2011**, *6* (2), No. e16641.
(59) Ramesh, M.; Campos, J. C.; Lee, P.; Song, Y.; Hernandez, G.; Sin, J.; Tucker, K. C.; Saadaeijahromi, H.; Gurney, M.; Ferreira, J. C.

https://doi.org/10.1021/acs.molpharmaceut.3c00508
Mol. Pharmaceutics 2023, 20, 5631−5645

B.; Andres, A. M. Mitophagy protects against statin-mediated skeletal muscle toxicity. *FASEB J.* **2019**, *33* (11), 11857−11869.
(60) Pascual Cruz, M.; Küstner, E. C.; Vicente, J. A. G.; Ferrero, X. M.; Thio, E. B.; López, J. L. Adverse side effects of statins in the oral cavity. *Med. Oral Patol Oral Cir Bucal* **2008**, *13* (2), E98−101.
(61) Říhová, B. Biocompatibility and immunocompatibility of water-soluble polymers based on HPMA. *Compos B: Eng.* **2007**, *38* (3), 386−397.
(62) Koppolu, P.; Sirisha, S.; Mishra, A.; Deshpande, K.; Lingam, A. S.; Alotaibi, D. H.; Alwahibi, M. S.; Penelag, S. Alkaline phosphatase and acid phosphatase levels in saliva and serum of patients with healthy periodontium, gingivitis, and periodontitis before and after scaling with root planing: A clinico-biochemical study. *Saudi J. Biol. Sci.* **2021**, *28* (1), 380−385.
(63) Malhotra, R.; Grover, V.; Kapoor, A.; Kapur, R. Alkaline phosphatase as a periodontal disease marker. *Indian J. Dent Res.* **2010**, *21* (4), 531−536.
(64) Bimstein, E.; Small, P. A., Jr.; Magnusson, I. Leukocyte esterase and protein levels in saliva, as indicators of gingival and periodontal diseases in children. *Pediatr Dent* **2004**, *26* (4), 310−315.

NOTE ADDED AFTER ASAP PUBLICATION

This paper was published ASAP on September 29, 2023. The author list for the paper should have had an additional author: Shabnam Arash. This was fixed in the version published ASAP on October 25, 2023.

https://doi.org/10.1021/acs.molpharmaceut.3c00508
Mol. Pharmaceutics 2023, 20, 5631−5645